Available online at www.sciencedirect.com
SCIENCE DIRECT
Polymer 47 (2006) 5997–6003
polymer
www.elsevier.com/locate/polymer

Swelling of polyelectrolyte hydrogels using a finite element model

R.A. Paxton, A.M. Al-Jumaily*

Diagnostics and Control Research Centre, Engineering Research Institute, Auckland University of Technology, 24 St. Paul Street, Auckland 1020, New Zealand

Received 3 April 2006; accepted 25 May 2006
Available online 30 June 2006

Abstract

In this work, a modular finite element model is proposed to describe the swelling of a poly(acrylic acid) hydrogel for optical applications under the influence of an electric field. The module divides the problem into five parts, depending on the specific energy domain involved. This includes electrical, chemical, force, mechanical and optical components. Each part is then solved sequentially to provide the final result. Initial predictions for the deformation are acceptable, and suggest that only a certain amount of energy may be available to deform the hydrogel during the swelling process.

Keywords: Finite element; Electroactive; Poly(acrylic acid)

1. Introduction

Polymer hydrogels are increasingly being used as alternative materials to the more conventional engineering materials in actuators and sensors. Some uses include artificial muscles [1], drug delivery [2] and temperature-sensitive actuators [3]. Our group has been studying these materials for several years as a novel type of changeable focal length (CFL) lens [4–8]. It is anticipated that if the swelling deformation and optical properties of polymer hydrogels are controlled, the deformation and low excitation voltage required for actuation would make these materials ideal for such an application.

Polyelectrolyte hydrogels, in particular poly(acrylic acid) (PAAC), are the main focus of this work, as the ionisable groups on their chains make them responsive to electrical stimulation. One problem that is encountered in this work is the lack of quantitative techniques to describe the swelling of polymer hydrogels. This has meant that significant time and resources have been spent in the laboratory performing experiments, some of which have later proved unnecessary. To counter that, work was begun to investigate methods for simulating experiments on a computer. Although some authors have already developed partial models to describe the swelling of polymer hydrogels [9–11], these models are complex and/or only focus on one particular part of the problems (for example, the ion flux through the hydrogel). Kenkare et al. [12] and deGennes et al. [13] proposed significantly simpler models and surprisingly, were able to obtain reasonable results. This suggests that although the processes involved in hydrogel swelling are complex, a macroscopic model may be able to provide useful results at a significantly lower computational cost.

None of the aforementioned models were designed with optical applications in mind, however, and so could not easily be used to describe hydrogel swelling for CFL applications. For this reason, this work attempts to build a fully descriptive macroscopic model capable of providing quantitative results within a short period of time. From the complexity of the equations involved, it was clear that the swelling of a hydrogel could not be solved analytically, and that numerical techniques need to be used. The mechanisms of hydrogel swelling were divided into blocks based on different energy domains [14], namely electrical, chemical, force, mechanical and optical (Fig. 1).

The Electrical module is the first part of the model, and is currently assumed to be time invariant. For this reason, it is

* Corresponding author. Tel. +64 9 921 9777; fax: +64 9 921 9973.
E-mail address: ahmed.al-jumaily@aut.ac.nz (A.M. Al-Jumaily).

0032-3861/$ - see front matter © 2006 Elsevier Ltd. All rights reserved.
doi:10.1016/j.polymer.2006.05.063

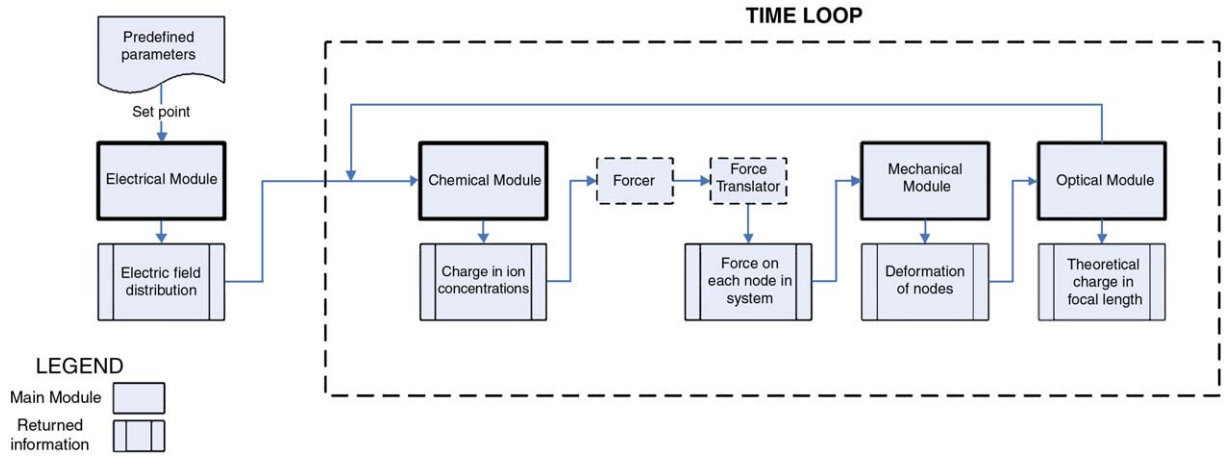

Fig. 1. Model divided into different energy domains.

placed outside the main timeloop, but could readily be added back into the loop if required. The module calculates the electric field that occurs in the hydrogel as a result of different electrode, hydrogel and solvent configurations. This field is then given to the Chemical module, which calculates the change in ion concentrations throughout the hydrogel. These changes in ion concentrations are known to cause osmotic pressure changes which are calculated by the Force module. The pressure (or force) is then given to the Mechanical module which calculates the resulting deformation of the hydrogel. The Optical module is the final module in the model, and interprets the output of the Mechanical module to provide the final change in focal length. Each of these modules will be discussed in more detail in the following sections.

The hydrogel studied in this work consists of circular disks of partially neutralised PAAC crosslinked with *N*,*N*-methylene-bis-acrylamide (BIS). The gels are formed using thermally triggered polymerisation techniques, and then placed into NaCl solution of varying concentrations. Electrodes are attached, and a voltage of between 1 and 5 V was applied with the resulting deformation recorded (as shown in Fig. 2).

2. Method of simulation

Although there are a variety of numerical methods available today, it was decided to implement this model using the finite element method (FEM). To simplify the resulting equations, this work utilises symmetry to generate a two-dimensional representation of the hydrogel/solvent system (Fig. 3). The hydrogel is modelled as a rectangle submerged in some fixed quantity of solvent. The level of solvent can be adjusted by altering this quantity. The system also comprises regions of air to the left and right sides of the gel, which act as 'no flux' boundaries. The domain is discretised using linear triangular elements, and then solved using both forward and central difference techniques. The model operates in a sequential form, although feedback methods are currently being investigated for future revisions.

2.1. Electrical module

The Electrical module is the first part in the model and it calculates the externally applied electric field in the hydrogel region. This module is based on the assumption that Laplace's equation in a conductor is equivalent to Kirchoff's current law (KCL). Based on this assumption, the Electrical module first assembles and then solves multiple, simultaneous instances of the KCL for each node in the system. This provides knowledge of the potential at each node, which the module can then use to calculate the externally applied electric field.

In order to simplify the calculations and increase the operation speed, the Electrical module makes a number of assumptions concerning the material and system properties. The

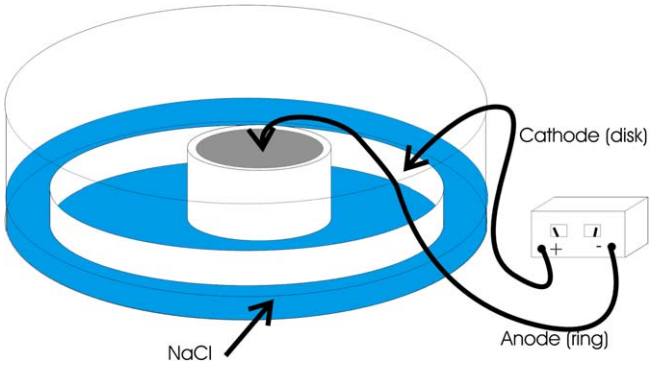

Fig. 2. Experimental setup modelled in this work.

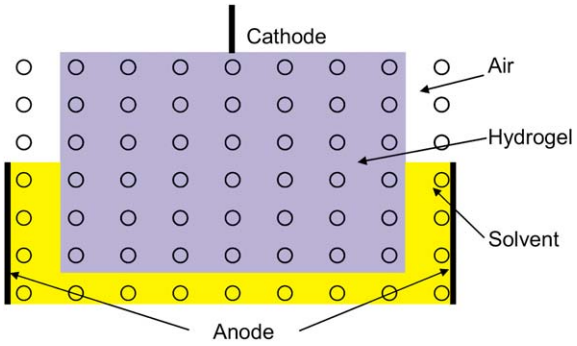

Fig. 3. Two-dimensional representation of hydrogel and solvent.

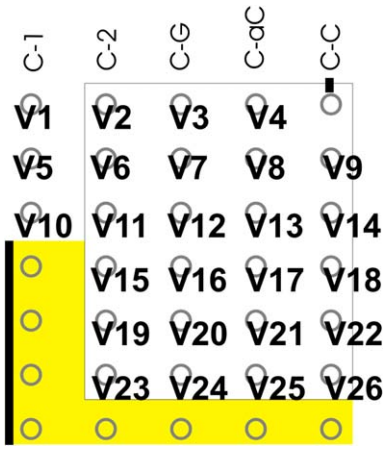

Fig. 4. Categorising nodes in hydrogel.

conductivity of the hydrogel is assumed to be homogeneous, unchanged during polymerisation and time invariant. Double-layer effects are also neglected. These assumptions allow much simpler forms of the KCL to be used in the model.

In its current form, the Electrical module is limited to solving only three well-defined electrode/hydrogel/solvent configurations. These are: (1) a single point cathode at the top of the hydrogel, with solvent around the sides of the gel only; (2) a single point cathode at the top of the hydrogel, with solvent around the sides and bottom of the gel; (3) a surface cathode that completely covers the top of the hydrogel, with solvent around the sides and bottom of the gel. The model can select any of these configurations, and can either perform the calculations in real time or prior to simulation (depending on the user's requirements). Although it was initially planned to allow the Electrical module to solve any given electrode configuration, this was later found to be impractical. By limiting the number of possible anode and cathode geometries, the Electrical module is able to categorise each node in the system into one of the following five kinds – first column of the system (C-1), second column of the system (C-2), general columns (C-G), column adjacent to the centre column (C-aC) and centre column (C-C) (as shown in Fig. 4). For example, consider a node at the edge of the hydrogel (e.g. node V2). Current will flow from the adjacent node (node V3) through node V2 and then to the node below it (node V6). For a centre node (e.g. node V20), current will flow from nodes V6 and V21 through this node towards nodes V19 and V24.

Using these different node classifications, the Electrical module first identifies the correct form of the KCL, and then assembles the different KCL equations for each node into a linear system (Fig. 5). The entire system is then solved

$$\begin{aligned} &V_1 + 2V_2 + 0V_3 \cdots + 0V_N = 0 \\ &0V_1 + V_2 + 0V_3 \cdots + 0V_N = V_{ANODE} \\ &V_1 + 0V_2 + 2V_3 \cdots + 0V_N = V_{ANODE} \\ &\vdots \\ &2V_1 + V_2 + V_3 \cdots + V_N = V_{CATHODE} \end{aligned} \longrightarrow \begin{pmatrix} 1 & 2 & 0 & \cdots & 0 \\ 0 & 2 & 0 & \cdots & 0 \\ 1 & 0 & 2 & \cdots & 0 \\ \vdots & \vdots & \vdots & \cdots & \vdots \\ 2 & 2 & 1 & \cdots & 1 \end{pmatrix} \begin{pmatrix} V_1 \\ V_2 \\ V_3 \\ \vdots \\ V_N \end{pmatrix} = \begin{pmatrix} V_1 \\ V_{ANODE} \\ V_{ANODE} \\ \vdots \\ V_{CATHODE} \end{pmatrix}$$

Fig. 5. Simultaneous KCL equations.

to provide a voltage potential for each node in the system. By definition, the electric field is defined as the gradient of the potential field, and so the Electrical module is able to calculate the externally applied field resulting from different electrode configurations. This field is then superimposed on the electric field that results from the movement of charged ions through the hydrogel region (and calculated by the Chemical module).

2.2. Chemical module

The Chemical module is the second part of the model, and also forms its main engine. It is responsible for calculating the temporal and spatial changes in ion concentrations, resulting from the diffusion and migration of each species, i. The Chemical module calculates the material flux by iteratively solving the two-dimensional diffusion equation:

$$\frac{\partial C_i}{\partial t} = D_i\left(\frac{\partial^2 C_i}{\partial x^2} + \frac{\partial^2 C_i}{\partial y^2}\right) + \frac{U_i}{|z_i|} z_i \left(\frac{\partial C_i}{\partial x} + \frac{\partial C_i}{\partial y}\right)\left(\frac{\partial \phi}{\partial x} + \frac{\partial \phi}{\partial y}\right) \quad (1)$$

where for each species, i, D is the diffusion coefficient, C is the concentration, U is the electrolytic mobility, z is the charge number, x and y are the system coordinates and ϕ is the electrostatic potential. The Chemical module solves Eq. (1) with a forward-difference time-integration scheme using Galerkin's method of weighted residual. In this model, linear triangular elements are used throughout, with the basis functions of these listed in Appendix A. Integrating the weighted residual of Eq. (1) over the domain, Ω, and boundary, Γ, and then simplifying to provide the weak form given by the integral, I:

$$\begin{aligned} I = &\int_\Omega w \frac{\partial C}{\partial t} \mathrm{d}\Omega + D_i \int_\Omega \left(\frac{\partial w}{\partial x}\frac{\partial C}{\partial x} + \frac{\partial w}{\partial y}\frac{\partial C}{\partial y}\right) \mathrm{d}\Omega \\ &- \frac{U_i}{|z_i|} z_i \int_\Omega \left(w\frac{\partial C}{\partial x} + w\frac{\partial C}{\partial y}\right)\left(\frac{\partial \phi}{\partial x} + \frac{\partial \phi}{\partial y}\right)\mathrm{d}\Omega - D_i \int_\Gamma w \frac{\partial C}{\partial n}\mathrm{d}\Gamma \end{aligned} \quad (2)$$

where w is the weighting function based on the shape functions. The fourth term in Eq. (2) describes the flux across the domain boundary, and in this model presented some challenges. As a result of the geometry of the hydrogel and solvent, regions of air are present to the sides of the hydrogel and above the solvent. Physically, no flux can pass into these regions, and thus 'no flux' boundary conditions need to be used. However, these conditions also meant that no flux could pass from the solvent region into the hydrogel, which is again unphysical. This model overcomes this difficulty by solving Eq. (2) twice during each timestep – once for the solvent region and again for the hydrogel region, where each of these regions has 'no flux' boundaries. Thus, applying 'no flux' boundaries and simplifying using integration by parts, Eq. (2) simplifies to an integral over the domain Ω only:

$$\left[M^{\mathrm{E}}\right]\left\{\begin{matrix}\dot{C}_1\\ \dot{C}_2\\ \dot{C}_3\end{matrix}\right\}^{t+\Delta t}+\left(\begin{matrix}D_i\left[K_1^{\mathrm{E}}\right]\\ -\dfrac{U_i}{|z_i|}z_i\left(\dfrac{\partial\phi}{\partial x}+\dfrac{\partial\phi}{\partial y}\right)\left[K_2^{\mathrm{E}}\right]\end{matrix}\right)\left\{\begin{matrix}C_1\\ C_2\\ C_3\end{matrix}\right\}^{t+\Delta t}=0 \tag{3}$$

where the matrices $[M^{\mathrm{E}}]$, $[K_1^{\mathrm{E}}]$ and $[K_2^{\mathrm{E}}]$ represent the mass and stiffness matrices (broken into two parts) for each element in the system. Since the Chemical module is implemented using a forward-difference time-integration scheme, the concentrations are calculated for the following timestep. The mass and stiffness matrices for each element are defined by different combinations of shape functions:

$$\left[M^{\mathrm{E}}\right]=\frac{\Delta}{12}\begin{bmatrix}2&1&1\\1&2&1\\1&1&2\end{bmatrix} \tag{4}$$

$$\left[K_1^{\mathrm{E}}\right]=\begin{bmatrix}\dfrac{\partial H_1^2}{\partial x^2}+\dfrac{\partial H_1^2}{\partial y^2} & \dfrac{\partial H_1\partial H_2}{\partial x^2}+\dfrac{\partial H_1\partial H_2}{\partial y^2} & \dfrac{\partial H_1\partial H_3}{\partial x^2}+\dfrac{\partial H_1\partial H_3}{\partial y^2}\\ \dfrac{\partial H_2\partial H_1}{\partial x^2}+\dfrac{\partial H_2\partial H_1}{\partial y^2} & \dfrac{\partial H_2^2}{\partial x^2}+\dfrac{\partial H_2^2}{\partial y^2} & \dfrac{\partial H_2\partial H_3}{\partial x^2}+\dfrac{\partial H_2\partial H_3}{\partial y^2}\\ \dfrac{\partial H_3\partial H_1}{\partial x^2}+\dfrac{\partial H_3\partial H_1}{\partial y^2} & \dfrac{\partial H_3\partial H_2}{\partial x^2}+\dfrac{\partial H_3\partial H_2}{\partial y^2} & \dfrac{\partial H_3^2}{\partial x^2}+\dfrac{\partial H_3^2}{\partial y^2}\end{bmatrix} \tag{5}$$

$$\left[K_2^{\mathrm{E}}\right]=\frac{\Delta}{3}\begin{bmatrix}\dfrac{\partial H_1}{\partial x}+\dfrac{\partial H_1}{\partial y} & \dfrac{\partial H_2}{\partial x}+\dfrac{\partial H_2}{\partial y} & \dfrac{\partial H_3}{\partial x}+\dfrac{\partial H_3}{\partial y}\\ \dfrac{\partial H_1}{\partial x}+\dfrac{\partial H_1}{\partial y} & \dfrac{\partial H_2}{\partial x}+\dfrac{\partial H_2}{\partial y} & \dfrac{\partial H_3}{\partial x}+\dfrac{\partial H_3}{\partial y}\\ \dfrac{\partial H_1}{\partial x}+\dfrac{\partial H_1}{\partial y} & \dfrac{\partial H_2}{\partial x}+\dfrac{\partial H_2}{\partial y} & \dfrac{\partial H_3}{\partial x}+\dfrac{\partial H_3}{\partial y}\end{bmatrix} \tag{6}$$

where Δ is the area of the element. The Chemical module first calculates the element matrices for each element in the domain, and then compiles these into global mass and stiffness matrices, $[M]$, $[K_1]$ and $[K_2]$:

$$[M]\left\{\begin{matrix}\dot{C}_1\\ \vdots\\ \dot{C}_n\end{matrix}\right\}^{t+\Delta t}+\left(\begin{matrix}D_i[K_1]\\ -\dfrac{U_i}{|z_i|}z_i\left(\dfrac{\partial\phi}{\partial x}+\dfrac{\partial\phi}{\partial y}\right)[K_2]\end{matrix}\right)\left\{\begin{matrix}C_1\\ \vdots\\ \dot{C}_n\end{matrix}\right\}^{t+\Delta t}=0 \tag{7}$$

where the concentration vectors, $\{C\}$ are now $1\times n$ elements long, with n as the total number of nodes in the system. Using the standard forward-difference equations, Eq. (7) can be rearranged to give:

$$\left([M]+[K]\Delta t\right)\left(C_i^{t+\Delta t}\right)=[M]\left(C_i^{t}\right) \tag{8}$$

which can then easily be solved for the concentration of each node for the following timestep. In Eq. (8), $[K]$ is equal to the sum of $[K_1]$ and $[K_2]$. In order to allow for reasonable computation times, this model only considers three species, namely mobile Na^+ ions (initially present in the hydrogel and solvent regions), mobile Cl^- ions (initially present in only the solvent region) and stationary COO^- ions fixed to the polymer chains (present only in the hydrogel region). As ions move from one region to another, they are assumed to carry water molecules with them, and it is this extra water that the model assumes generates the swelling of the hydrogel.

2.3. Force module

The Force module is the third part in the model and acts as an interface between the Chemical and Mechanical modules. This was found to be necessary as the Mechanical module requires force as an input, but the Chemical module only calculates the change in ion concentrations (Eq. (1)). Using these changes in ion concentrations, the Force module calculates the osmotic pressure (force) on the hydrogel generated by the differences in the chemical potential between the hydrogel and solvent regions.

Currently, the Force module analyses the swelling behaviour of polymer hydrogels within the framework of the Flory–Rehner (F–R) theory [15], the main basis of which is the osmotic pressure (π). Although the F–R theory is generally regarded as only being accurate for ideal cases, most gel swelling models also utilise it and so it is used in this model. According to the F–R theory, the total osmotic pressure on the hydrogel can be considered to be made up of three terms: the osmotic pressure due to ionic interactions (π_{ion}), the osmotic pressure due to polymer/solvent mixing (π_{mix}) and the osmotic pressure due to the elasticity of the polymer chains (π_{elas}). These can be written as:

$$\pi_{\mathrm{ion}}=\mathrm{R}T\sum_i\left(C_i^{\mathrm{G}}-C_i^{\mathrm{S}}\right) \tag{9}$$

$$\pi_{\mathrm{mix}}=-\frac{\mathrm{R}T}{V_{\mathrm{S}}}\left[\ln(1-v_{\mathrm{P}})+v_{\mathrm{P}}+\chi v_{\mathrm{P}}^2\right] \tag{10}$$

$$\pi_{\mathrm{mix}}=-\frac{\mathrm{R}T}{V_{\mathrm{S}}}N^{-1}\left(v_{\mathrm{P}}^{1/3}v_0^{2/3}-v_{\mathrm{P}}/2\right) \tag{11}$$

where R is the molar gas constant, T is the temperature, C_i^{G} and C_i^{S} are the concentrations of mobile species i in the hydrogel and solvent regions, V_{S} is the volume of solvent, v_{P} is the volume fraction of polymer in the hydrogel, χ is the Flory–Huggins interaction parameter, N is the average number of segments in the network and v_0 is the volume fraction of the network after synthesis. In this model, the elastic restoring

force generated by the polymer chains is calculated in the Mechanical module, and so Eq. (11) is not used in the Force module. It is also important to note that these three osmotic pressures are not equally applied to every node in the system – for example, Eq. (9) has terms for the concentration in both the solvent and hydrogel regions, and so this model acts at the gel/solvent boundary. The osmotic pressure due to polymer/solvent mixing is applied to every node in the system, however, as this pressure serves to expand the overall gel. This idea is illustrated in Fig. 6.

During each timestep, the Force module uses the change in ion concentrations (calculated by the Chemical module) to calculate the resulting osmotic pressure on each node in the system. With knowledge of the dimensions and surface areas of the hydrogel region, the Force module then converts this osmotic pressure into a force on each node. The resulting force vector is then used as input for the Mechanical module.

2.4. Mechanical module

The Mechanical module is the penultimate part of the model, but is the final module that provides results needed by the other modules. This module receives information about the magnitude, direction and location of forces being applied to the hydrogel from the Force module. The Mechanical module then calculates the predicted nodal deformations resulting from these forces, which can be displayed graphically. The basis of the Mechanical module is the standard equation of dynamic motion:

$$[M]\{\ddot{d}\}^t+[K]\{d\}^t=\{F\}^t \tag{12}$$

where $[M]$ and $[K]$ are the mass and stiffness matrices, $\{F\}$ is a vector of input forces and $\{d\}$ is the displacement of the nodes (Fig. 7). In this model, any damping is neglected.

The mass matrix in Eq. (12) provides the inertial term in the equation, and its exact form depends on the shape functions of the elements used. In this model, all of the module utilise the same shape functions for linear triangular elements, which are given in Appendix A. For each element, the mass matrix is given by:

$$\left[M^{\mathrm{E}}\right]=\int_{\Omega^{\mathrm{e}}}[N]^{\mathrm{T}}\rho[N]\mathrm{d}\Omega \tag{13}$$

where the integral is taken over the entire element area. ρ is the mass density and $[N]$ is given by:

$$N=\begin{bmatrix}H_1 & 0 & H_2 & 0 & H_3 & 0\\ 0 & H_1 & 0 & H_2 & 0 & H_3\end{bmatrix} \tag{14}$$

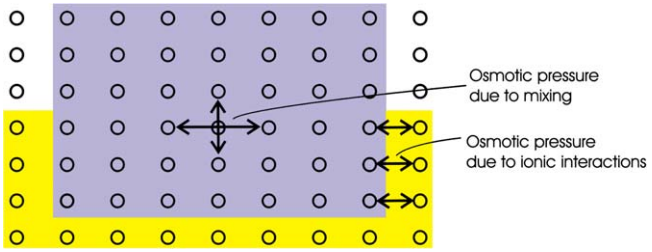

Fig. 6. Osmotic pressure due to ionic interactions and mixing.

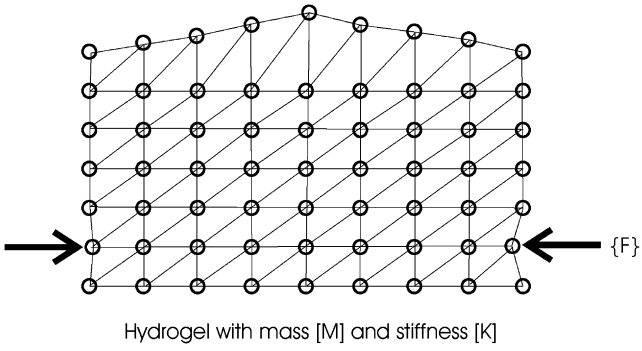

Fig. 7. Forces acting on hydrogel deform material.

Eq. (13) can be simplified to give the more common form of the mass matrix:

$$\left[M^{\mathrm{E}}\right]=\frac{\rho A}{12}\begin{bmatrix}2 & 0 & 1 & 0 & 1 & 0\\ 0 & 2 & 0 & 1 & 0 & 1\\ 1 & 0 & 2 & 0 & 1 & 0\\ 0 & 1 & 0 & 2 & 0 & 1\\ 1 & 0 & 1 & 0 & 2 & 0\\ 0 & 1 & 0 & 1 & 0 & 2\end{bmatrix} \tag{15}$$

which is known as the consistent mass matrix. Eq. (13) can also be substituted with the lumped mass matrix which can be easier to implement.

The element stiffness matrix provides the elastic response of the hydrogel, which in this model is assumed to obey linear elasticity. The element stiffness matrix is given by:

$$[K_{\mathrm{E}}]=\frac{1}{2}\int_{\Omega^{\mathrm{e}}}\{\sigma\}^t\{\varepsilon\}\,\mathrm{d}\Omega \tag{16}$$

where σ is the stress and ε is the strain, integrated over the entire element area (Ω). In linear elasticity, the strain in the element is related to the nodal displacement, $\{u\}$ through:

$$\{\varepsilon\}=[\mathbf{B}]\{u\} \tag{17}$$

where $[\mathbf{B}]$ is the kinematic matrix, which is again dependent on the shape functions of the elements used:

$$[\mathbf{B}]=\frac{1}{2A}\begin{bmatrix}(y_2-y_3) & 0 & (y_3-y_1) & 0 & (y_1-y_2) & 0\\ 0 & (x_3-x_2) & 0 & (x_1-x_3) & 0 & (x_2-x_1)\\ (x_3-x_2) & (y_2-y_3) & (x_1-x_3) & (y_3-y_1) & (x_2-x_1) & (y_1-y_2)\end{bmatrix} \tag{18}$$

where (x_i, y_i) are the x- and y-coordinates of the ith element node. In an isotropic material with plane stress, the element strains are also related to their respective two-dimensional stresses through Hook's law:

$$\{\sigma\} = [\mathbf{D}]\{\varepsilon\} \tag{19}$$

where [**D**] is a material property matrix that depends on the Young's modulus and Poisson ratio for the material:

$$[\mathbf{D}] = \frac{E}{1-\nu^2}\begin{bmatrix} 1 & \nu & 0 \\ \nu & 1 & 0 \\ 0 & 0 & \dfrac{1-\nu}{2} \end{bmatrix} \tag{20}$$

where E is the Young's modulus and ν is Poisson's ratio.

Once the Mechanical module has calculated the mass and stiffness matrices for each element in the hydrogel domain, these are assembled into the global mass and stiffness matrices given in Eq. (12). Eq. (12) can rapidly be rearranged to allow the Mechanical module to solve for the acceleration of each node:

$$\{\ddot{d}\}^t = [M]^{-1}(\{F\}^t - [K]\{d\}^t) \tag{21}$$

where $\{\ddot{d}\}^t$ is the acceleration, $\{F\}^t$ is the applied force and $\{d\}^t$ is the displacement at the current timestep. The displacement for each node in the system for the following timestep can then be calculated by using the current nodal displacement and velocity:

$$\{d\}^{t+\Delta t} = \{d\}^t + \Delta t\{\dot{d}\}^{t+0.5\,\Delta t} \tag{22}$$

where Δt is the size of the timestep. In this model, the mass and stiffness matrices are assumed to be time invariant as this reduces the complexity of the equations that need to be solved by the Mechanical module. This assumption is justified by the fact that the hydrogel behaves linearly in quasistatic situations and because the hydrogel is extremely elastic. Real poly(acrylic acid) hydrogels are known to consist of regions of high and low density [16], however, which cause spatial variations in the hydrogel elasticity. Real hydrogels also possess viscoelastic properties (and not purely elastic) which cause hysteresis effects. Some hydrogels can also vary their elasticity under the influence of an electric field [17] which further complicates material assumptions. The integration of these ideas into this model is ongoing, and will provide better future results.

2.5. Optical module

The Optical module is the final component in the overall model and returns the final result of the model (a change in focal length). It takes as its input the deformation calculated by the Mechanical module and then curve-fits this to either a parabolic or circular surface to calculate the theoretical radius of curvature and refractive power (Fig. 8).

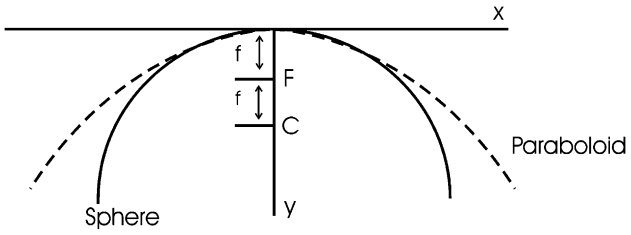

Fig. 8. Comparison of circular and parabolic curve fits.

While the Mechanical module calculates the deformation of each node in the system, the Optical module currently only uses the deformation of the upper, centre and right nodes. The deformation of each of these nodes is calculated, and then the curve fitted to provide the radius of curvature (Fig. 9). The relationship between the deformation (Δy) and radius of curvature (R) for a parabolic fit is given by:

$$R = \frac{x^2}{2\Delta y} \tag{23}$$

For a circular fit, the relationship between the deformation and radius of curvature is given by:

$$R = \frac{x^2 + 4\Delta y^2}{8\Delta y} \tag{24}$$

While these approximations may appear simplistic, in practise they do provide reasonable results for the change in the radius of the curvature. Future developments on this model will improve the curve-fitting capabilities to include aspherical curve fits. Future work on the Optical module will also incorporate information on the refractive index to allow theoretical focal length calculations to be made.

3. Initial simulation results

Simulations were run for systems using two different electrode configurations, and predicted deformation of the upper left, centre and right nodes are shown in Fig. 10. For all three nodes, the model predicts that the rate of hydrogel swelling does not depend on the applied voltage, and that the deformation grows exponentially to some maximum value. Furthermore, the model predicts that deformation of the centre node increases with increasing voltage, but the deformation of the left and right nodes decreases with increasing voltage. This suggests that there may only be a finite amount of energy available to deform the hydrogel. Experimental validation of the model is currently underway, and should provide insight into any limitations of this model.

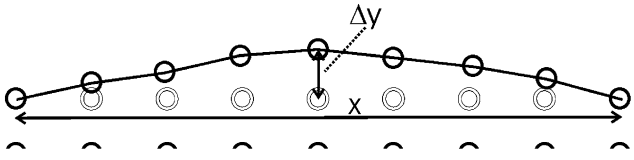

Fig. 9. Curve fitting the deformation of the upper surface.

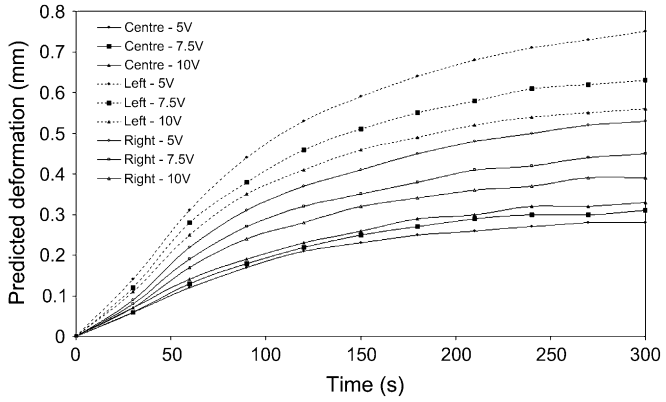

Fig. 10. Predicted deformation of the upper surface nodes.

4. Conclusion

The model introduced in this work represents a significant departure from the methods normally used to solve hydrogel swelling problems. The overall gel swelling process is broken into different parts (modules) depending on their respective energy domains. Each module can then be solved independently of each other, and the results superimposed to provide the final answer. This can be achieved quickly and efficiently, and has the advantage that each module can be improved or modified independently. The model makes interesting predictions for the swelling rate and final deformations of the nodes, which are in the process of being validated experimentally.

Appendix A

Linear triangular elements are used throughout this model in both the Chemical and Mechanical modules. Linear triangular elements each have three nodes, and so have the corresponding shape functions:

$$H_1 = \frac{1}{2A}[(x_2y_3 - x_3y_2) + (y_2 - y_3)x + (x_3 - x_2)y]$$
$$H_2 = \frac{1}{2A}[(x_3y_1 - x_1y_3) + (y_3 - y_1)x + (x_1 - x_3)y] \quad (25)$$
$$H_3 = \frac{1}{2A}[(x_1y_2 - x_2y_1) + (y_1 - y_2)x + (x_2 - x_1)y]$$

where (x_i, y_i) are the x- and y-coordinates of the ith element node and A is the area.

References

[1] Ashley S. Scientific American 2003:53–60.
[2] Sen M, Guven O. Computational and Theoretical Polymer Science 2001; 11:475–82.
[3] Hu Z, Li Y. Proceedings of SPIE 1996;2716:224–30.
[4] Paxton RA. Master of Engineering thesis. Auckland: Auckland University of Technology; 2002.
[5] Paxton R, Al-Jumaily AM, Easteal AJ. Polymer Testing 2003;22:371–4.
[6] Paxton R, Al-Jumaily AM, Easteal AJ. Proceedings of SPIE 2003;5051:504–8.
[7] Paxton R, Al-Jumaily AM, Easteal AJ. In: Proceedings of the ninth annual New Zealand engineering and technology postgraduate conference, vol. 1; 2002. p. 33–7.
[8] Sakhawat M, Al-Jumaily AM, Naidu LS, Dodd DM. In: Proceedings of the seventh annual New Zealand engineering and technology postgraduate conference, vol. 1; 2000. p. 257–81.
[9] Achilleous EC, Prud'homme RK, Kevrekidis IG. Fluid Mechanics and Transport Phenomena 2000;46(11):2128–39.
[10] Achilleous EC, Christodoulou KN, Kevrekidis IG. Computational and Theoretical Polymer Science 2001;11:63–80.
[11] Wallmersperger T, Kroplin B, Gulch R. In: SPIE, vol. 4695, San Diego, California, USA; 2002.
[12] Kenkare NR, Hall CK, Khan SA. Journal of Chemical Physics 2000; 113(1):404–18.
[13] deGennes PG, Okumura KO, Shahinpoor M, Kim KJ. Europhysics Letters 2000;50(4):513–8.
[14] Lee W. PhD thesis, Department of Mechanical Engineering. Boston: Massachusetts Institute of Technology; 1996.
[15] Durmaz S, Okay O. Polymer 2000;41:3693–704.
[16] Pekcan Ö, Kara S. Polymer 2000;41:8735–9.
[17] Shiga T. Advances in Polymer Science 1997;134:131–63.